BIOCHEMISTRY
including biophysical chemistry & molecular biology

Article

pubs.acs.org/biochemistry

Caveolin-1 Is a Competitive Inhibitor of Heme Oxygenase-1 (HO-1) with Heme: Identification of a Minimum Sequence in Caveolin-1 for Binding to HO-1

Junichi Taira,[†] Masakazu Sugishima,[‡] Yutaka Kida,[§] Eriko Oda,[†] Masato Noguchi,[‡] and Yuichiro Higashimoto*,[†]

[†]Department of Chemistry, [‡]Department of Medical Biochemistry, and [§]Division of Microbiology, Department of Infectious Medicine, Kurume University School of Medicine, Kurume 830-0011, Japan

ABSTRACT: Heme oxygenase (HO) catalyzes the O_2-dependent degradation of heme to biliverdin IXα, carbon monoxide (CO), and free ferrous iron through a multistep mechanism. Electrons required for HO catalysis in mammals are provided by NADPH−cytochrome P450 reductase. Recently, Kim et al. reported for the first time that HO, especially inducible HO-1, appears in caveolae and showed that caveolin-1, a principal isoform of the caveolin family, physically interacts with HO-1 [Jung, N. H. et al. (2003) *IUBMB Life 55*, 525−532 ; Kim, H. P. et al. (2004) *FASEB J. 18*, 1080−1089]. In the present study, we confirmed by immunoprecipitation experiments that rat HO-1 and rat caveolin-1 (residues 1−101) directly interact with each other and that the HO-1 activity is inhibited by caveolin-1 (1−101). The 82−101 residues of caveolin-1 (CAV(82−101)), called the caveolin scaffolding domain, play essential roles in caveolin-related protein−protein interactions. The HO-1 activity is also inhibited by CAV(82−101) in a competitive manner with hemin, and a hemin titration experiment showed that CAV(82−101) interferes with hemin binding to HO-1. The enzyme kinetics and surface plasmon resonance experiments gave comparable K_i and K_D values of 5.2 and 1.0 μM for CAV(82−101), respectively, with respect to the interaction with HO-1. These observations indicated that CAV(82−101) and hemin share a common binding site within the HO-1 protein. The identified caveolin binding motif (FLLNIELF) of rat HO-1 is incomplete compared to the proposed consensus sequence. The affinity between HO-1 and CAV(82−101), however, was almost completely or remarkably eliminated by replacement of Phe^{207} and/or Phe^{214} with Ala, indicating that HO-1 binds to caveolin-1 via this motif. Among the peptide fragments derived from CAV(82−101), i.e., CAV(82−91), CAV(87−96), CAV(92−101), and CAV(97−101), CAV(92−101) and CAV(97−101) are able to inhibit the HO-1 activity to a similar extent; thus, the five-amino acid sequence (residues 97−101) is considered to be a minimum sequence for binding to HO-1.

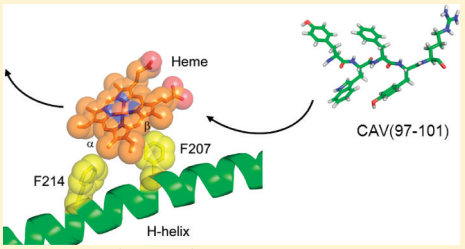

Heme oxygenase (HO, EC 1.14.99.3) catalyzes the O_2-dependent degradation of heme to biliverdin IXα, carbon monoxide (CO), and free ferrous iron through a multistep mechanism.[1,2] Electrons required for HO catalysis in mammals are provided by NADPH−cytochrome P450 reductase (CPR, EC 1.6.2.4), a flavoprotein containing one molecule each of FAD and FMN.[3−5]

Two isoforms, an inducible form, HO-1,[6] and a constitutive form, HO-2,[7] have been identified in mammalian cells. HO-1 is mainly expressed in liver, spleen, and macrophages and is in charge of physiological heme degradation derived from senescent erythrocytes. Biliverdin generated in the HO reaction is converted to bilirubin by a cytoplasmic enzyme, biliverdin reductase (BVR). Bilirubin is well-known as a strong antioxidant *in vivo*. Thus, it is believed that HO-1 plays an essential role in cellular and tissue protections against oxidative stresses. In fact, HO-1 is induced by various types of oxidative stress.[8]

On the other hand, HO-2 is constitutively expressed especially in the neurovascular system and is thought to be involved in signaling processes via CO. A physiological signaling role for CO was first suggested from observations that CO can weakly stimulate soluble guanylyl cyclase (sGC) *in vitro* by heme binding to produce cGMP.[9,10] Since then, ample, though circumstantial, evidence has been accumulated with respect to HO-derived CO as a novel gaseous signal mediator.[11−13] Nonetheless, unequivocal roles for sGC in signaling processes triggered by CO have not been established.

To understand CO-mediated signal transduction, it will be important to elucidate the regulating system of CO production. Since CO is highly stable compared to nitric oxide (NO), CO would accumulate in the signaling pathway if CO production is not appropriately controlled; accumulation of CO *in vivo* might cause carbon monoxide poisoning, including anoxia. Therefore, HO activity should be strictly controlled at the protein level. It has been reported that overexpression of HO in ECV304 cells or hamster fibroblasts paradoxically enhanced susceptibility of the cells to oxidative injury.[14,15] Thus, it is conceivable that a modulating system of HO activity could be functioning *in vivo*. Thus far, however, such a system has not been extensively explored.

Recently, Kim et al. reported compartmentalization of HO-1 into caveolae in mouse mesangial cells[16] and rat endothelial

Received: April 19, 2011
Revised: June 8, 2011
Published: July 2, 2011

cells;[17] caveolae are vesicular invaginations of the plasma membrane, and the chief structural proteins of caveolae are caveolins. Caveolins are a group of 21−24 kDa integral membrane proteins; molecular cloning has identified three distinct caveolin genes: caveolin-1,[18] caveolin-2,[19] and caveolin-3.[20] Caveolins form a scaffold onto which a variety of signaling molecules can assemble to generate preassembled signaling complexes.[21] Caveolin-1 is the major isoform of caveolins and is expressed abundantly in endothelial cells. Caveolin-1 has two cytosolic domains (1−104 and 126−178 residues) separated by a membrane-integral domain (105−125 residues), and three Cys residues at the C-terminal cytosolic domain are palmitoylated. It is known that caveolin-1 regulates caveolae-related signaling processes.[21,22] In general, the interactions of signaling molecules with caveolin-1 through its N-terminal cytosolic domain generate inhibitory effects on signaling molecules.

With respect to HO-1, Kim et al. reported (i) HO activity, especially the inducible isoform, appears in plasma membrane, cytosol, and isolated caveolae; (ii) caveolin-1 physically interacts with HO-1; (iii) HO activity dramatically increases in cells expressing caveolin-1 antisense transcripts; and (iv) conversely, caveolin-1 expression attenuates lipopolysaccharide-induced HO activity.[17] Since the discovery of HO by Schmid and co-workers in the 1960s, HO has been described as an endoplasmic reticulum-associated protein.[3,6] Kim et al. demonstrated for the first time the localization of heme degradation enzymes, i.e., HO, CPR, and BVR, to caveolae and presented novel evidence that caveolin-1 interacts with HO[16] and modulates HO activity.[17]

Caveolin-1 interacts with many signaling proteins that contain the caveolin binding motifs ΦXΦXXXXΦ or ΦXXXXΦXXΦ (Φ is Phe, Tyr, or Trp).[23−27] The possible caveolin binding motif, FEYNMQIF (residues 227−234), is identified in human HO-2, but the corresponding sequence in human HO-1, FLLNIQLF (residues 207−214), seems to be incomplete compared to the above-defined binding motifs. Despite this incompleteness, reports indicating an inhibitory effect of caveolin-1 on HO-1 have steadily accumulated.[16,17,28−30] NO synthase (NOS), a pivotal enzyme in NO signaling, was also recognized as one of the caveolin interacting proteins more than a decade ago.[27,31−33] Functional similarities are found between HO and NOS oxygenase domains, such as heme binding and NADPH-dependent oxygenase activity. The oxygenase domain of NOS contains the caveolin binding motif and indeed sustains the inhibitory effect of caveolin-1.[27,34] Mutational experiments, however, showed the motif is not necessarily required for the inhibition of NOS activity.[35,36] These findings suggest that caveolin-1 may interact with proteins in which the binding motif is incomplete or absent and that modulating mechanisms by caveolin-1 may be different among caveolin interacting proteins.

Thus, caveolin-1 may function as an endogenous modulator of HO-1. In the present study, we probed the molecular interaction between HO-1 and caveolin-1 and attempted to characterize the binding property between them and to specify the core binding sequences in both proteins.

EXPERIMENTAL PROCEDURES

Materials. Oligonucleotides for PCR amplification and mutageneses were obtained from FASMAC (Atsugi, Japan). Anti-HO-1 and anti-caveolin-1 antibodies used for immunoprecipitation and immunoblotting experiments were purchased from Promega (Madison, WI) and Cell Signaling Technology (Beverly, MA), respectively, and horseradish peroxidase (HRP)-conjugated anti-rabbit IgG antibody was obtained from Santa Cruz Biotechnology (Santa Cruz, CA). Rat caveolin-1-derived peptides were synthesized by conventional 9-fluorenylmethoxycarbonyl (Fmoc) chemistry.[37] Purity and homogeneity of the peptides were confirmed by RP-HPLC and MALDI-TOF MS. A synthetic peptide corresponding to the residues 82−101 of rat caveolin-1 (DGIWKASFTTFTVT-KYWFYR-amide) is designated as CAV(82−101). Correspondingly, CAV(82−91) (DGIWKASFTT-amide), CAV(87−96) (ASFTTFTVTK-amide), CAV(92−101) (FTVTKYWFYR-amide), and CAV(97−101) (YWFYR-amide) are collectively referred to as fragments of CAV(82−101). A L-Cys-conjugated variant of CAV(82−101) with a spacer of 6-aminohexanoic acid (Ahx), Cys-Ahx-CAV(82−101), was also prepared by Fmoc chemistry and used for affinity chromatography. Other chemicals of reagent grade were obtained from Sigma (Tokyo, Japan), Wako Pure Chemicals (Osaka, Japan), or Nacalai Tesque (Kyoto, Japan).

Preparation of Constructs. Since the primary structures of HO-1 and caveolin-1 are highly conserved among mammalian species, rat HO-1 and rat caveolin-1 were used in the present study. The expression vector of rat HO-1, HO-1/pBAce,[38] was used to obtain a soluble form of rat HO-1 lacking the 22-amino acid C-terminal transmembrane region; hereafter this truncated rat HO-1 (1−267) is referred to as tHO-1 (truncated HO-1). The cDNA encoding rat caveolin-1 (1−101) was cloned by PCR from rat liver cDNA library (Clontech, Mountain View, CA). The cDNAs of tHO-1 excised from HO-1/pBAce and caveolin-1 (1−101) were subcloned into pcDNA3.1D/V5-His-TOPO (Invitrogen, Carlsbad, CA) for expression in COS-7 cells (American Type Culture Collection, Manassas, VA) as His_6-tagged proteins. The cDNAs of tHO-1 and caveolin-1 (1−101) were also subcloned into NdeI-BamHI sites of the pET15b (Novagen, Darmstadt, Germany) and NdeI-XhoI sites of pET21b (Novagen), respectively, for expression in *Escherichia coli* (*E. coli*) as His_6-tagged proteins. In order to obtain constructs of tHO-1 mutants (F207A, F214A, and F207A/F214A), the HO-1/pBAce vector[38] was mutated using QuikChange site-directed mutagenesis kit (Stratagene, La Jolla, CA).

Immunoprecipitation. The COS-7 cells were maintained in high-glucose Dulbecco's modified Eagle medium with 10% fetal bovine serum, 100 U/mL of penicillin, and 100 μg/mL of streptomycin and cultured at 37 °C in a humidified atmosphere containing 5% CO_2. For expression of tHO-1 and caveolin-1 (1−101) with His_6-tag, the tHO-1/pcDNA3.1D/V5-His-TOPO and caveolin-1 (1−101)/pcDNA3.1D/V5-His-TOPO were separately transfected into the COS-7 cells with FuGENE 6 (Roche Diagnostics, Basel, Switzerland). For coexpression of the two proteins, both vectors were cotransfected into the cells. Cell culture was continued for 48 h up to 80% confluence. After rinsing twice with phosphate-buffered saline, cells were harvested and lysed with 50 mM Tris-HCl buffer (pH 8.0) containing 1% Triton X-100, 5 mM EDTA, and a protease inhibitors cocktail (Complete, Mini, EDTA-free, Roche Diagnostics). The cell lysates were incubated with antibody-conjugated beads overnight at 4 °C; anti-HO-1 antibody-immobilized protein A-Sepharose (Sigma) was employed for tHO-1, and anti-caveolin-1 antibody-conjugated agarose

(Santa Cruz) was used for caveolin-1 (1−101). After washing the beads with the lysis buffer, the proteins bound to the beads were subjected to SDS-PAGE under reducing conditions and transferred to nitrocellulose membrane. The membrane was placed in a blocking solution (Nacalai Tesque) for 1 h and incubated for an additional hour with the primary antibodies. After washing with phosphate-buffered saline with 0.1% Tween 20 (PBST), the membrane was incubated with the HRP-conjugated secondary antibody for 30 min. Bound IgG was visualized by ECL advance (GE Healthcare, Buckinghamshire, UK) and analyzed with LAS 4000 (GE Healthcare). Monoclonal anti-polyhistidine antibody (Sigma) was employed to detect the His_6-tagged proteins.

Expression and Purification of the Recombinant Proteins. The constructs, tHO-1/pET15b and caveolin-1 (1−101)/pET21b, were separately introduced into *E. coli* BL21(DE3) (Novagen), and cells were grown in LB broth containing 100 μg/mL ampicillin. The recombinant proteins were overexpressed with 1 mM isopropyl β-D-thiogalactoside for 3 h at 37 °C with aeration. Cells were harvested by centrifugation (8000 rpm, 30 min). The cell pellet containing tHO-1 was resuspended in 50 mL of extraction buffer consisting of 50 mM Tris-HCl (pH 8.0), 0.2 mg/mL lysozyme, and Complete, Mini, EDTA-free, incubated for 1 h, lysed by sonication and centrifuged (12000 rpm, 30 min). Because caveolin-1 (1−101) was trapped in inclusion bodies, the pellet containing caveolin-1 (1−101) was lysed with 8 M urea and centrifuged. These His_6-tagged proteins were purified with a Ni Sepharose 6 Fast Flow column (GE Healthcare) and a HiTrap Q HP column (GE Healthcare) on ÄKTAprime plus (GE Healthcare); the Ni Sepharose column (1 mL bed volume) had been equilibrated with 20 mM Tris-HCl (pH 8.0) containing 25 mM imidazole and 150 mM KCl and was eluted with 20 mM Tris-HCl (pH 7.4) containing 250 mM imidazole; the HiTrap Q HP column (1 mL bed volume) had been equilibrated with 20 mM Tris-HCl (pH 7.4) and was eluted with a 60 mL linear gradient between 20 mM Tris-HCl (pH 7.4) and 20 mM Tris-HCl (pH 7.4) plus 400 mM KCl. The expression vectors (F207A/pBAce, F214A/pBAce, and F207A/F214A/pBAce) of the mutant proteins (F207A, F214A, and F207A/F214A) were separately introduced into *E. coli* JM109 (Toyobo, Osaka, Japan), and the proteins were expressed by lowering the phosphate concentration in the medium and then purified by a HiTrap Q HP column (GE Healthcare) as previously described.[38]

The purified recombinant proteins were concentrated and desalted with Amicon Ultra-15 (Millipore, Billerica, MA); the purity of the proteins was confirmed by SDS-PAGE, and their concentrations were determined by bicinchoninic acid protein assay.

***In Vitro* Binding Assay of tHO-1 to Cys-Ahx-CAV(82−101).** tHO-1 solution (10 μM) was applied to a column (1 mL bed volume) of Cys-Ahx-CAV(82−101)-immobilized Sulfo-Link Coupling Gel (Pierce, Rockford, IL) equilibrated with 50 mM Tris-HCl (pH 8.5) containing 5 mM EDTA. After washing the column with the same buffer, tHO-1 bound to the gel was eluted with 6 M urea. Control experiment was performed by the same procedures using a L-Cys-immobilized column. The tHO-1 in the eluate was analyzed by Western blotting and visualized as described above.

Assay of Heme Oxygenase Activity. The HO activity was determined by the rate of bilirubin formation. Assay was carried out according to the method reported previously.[39] Briefly, the assay mixture (200 μL) contained 2, 4, or 20 μM hemin, 0.38 μM BVR, 1.6 μM CPR, 3×10^3 unit catalase, 0.5 mg/mL bovine serum albumin, 2.3 μg (0.38 μM) of tHO-1 or F207A/F214A, and 100 mM potassium phosphate buffer (pH 7.4). The assay mixture was preincubated in the presence or absence of varied concentrations of caveolin-1 (1−101) or CAV(82−101) at 4 °C for 30 min. Then the reaction was started by addition of NADPH (final 100 μM). The rate of bilirubin formation was measured from the increase of absorbance at 468 nm using a Cary 50 Bio UV/vis spectro photometer (Varian, Palo Alto, CA). The HO activities were also assayed in the presence of the fragments of CAV(82−101) where indicated.

Titration of tHO-1 with Hemin. The hemin stock solution (50 μM) was prepared in 0.1 M potassium phosphate buffer (pH 7.4); its concentration was determined by the pyridine hemochrome method.[40] tHO-1 (5 μM) in 0.1 M potassium phosphate buffer (pH 7.4) was preincubated with varied concentrations (0, 25, and 50 μM) of CAV(82−101) for 30 min at 4 °C before titration. The titration solution (200 μL) was transferred into a quartz cuvette (1 cm path length), and tHO-1 was titrated at 25 °C by consecutive additions of 2 μL each of the hemin stock solution. After each addition, absorption spectra from 300 to 600 nm were recorded. Titration of F207A/F214A with hemin was done under the same conditions without CAV(82−101).

Surface Plasmon Resonance (SPR) Measurement. CAV(82−101) was dissolved in 10 mM sodium acetate (pH 4) and immobilized via the amino groups to CM5 sensor chip (GE Healthcare) with the aid of 1-ethyl-3-(3-dimethylaminopropyl)-carbodiimide and *N*-hydroxysuccinimide. As a optimal immobilization level, about 100 response units were selected. For affinity measurements, the association and dissociation phases were monitored in a BIAcore 1000 (GE Healthcare).[41] The analytes, tHO-1, F207A, F214A, and F207A/F214A, which were dissolved in HBS-EP running buffer (GE Healthcare), were injected into the flow cell at concentrations of 0.5, 1.0, and 2.0 μM at a flow rate of 10 μL/min at 25 °C. The sensor chip was regenerated with pulses of 20 mM Tris-HCl buffer (pH 8.0) containing 6 M urea to the baseline level, followed by an extensive washing with the running buffer. Control experiments were performed with the caveolin peptide-free channel on the same sensor chip. From the assay curves obtained, the control signals, reflecting the bulk effect of buffer, were subtracted using BIA-evaluation 4.1 software (GE Healthcare). The association (k_a) and dissociation (k_d) rate constants were determined using the equation for 1:1 Langmuir binding. Equilibrium dissociation constants (K_D) were calculated from mean values of the obtained rate constants.

RESULTS

Construction and Expression of Caveolin-1 (1−101). Caveolin-1 exerts protein−protein interaction through its N-terminal cytosolic domain (1−101 residues).[23,42] Hence, caveolin-1 (1−101) was used for *in vivo* and *in vitro* experiments by removal of the membrane-integral domain and C-terminal cytosolic domain of caveolin-1 (102−178 residues). Caveolin-1 (1−101) expressed in *E. coli* was trapped in inclusion bodies. Therefore, we extracted caveolin-1 (1−101) from the inclusion bodies by treatment with 8 M urea. Fernandez et al. reported that caveolin-1 (1−101) does not

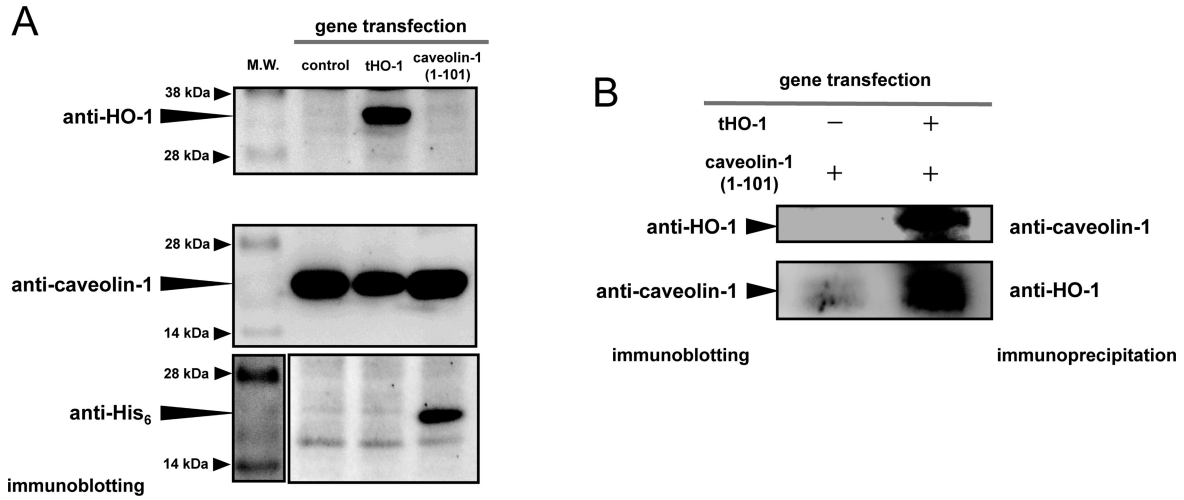

Figure 1. Interaction of tHO-1 and caveolin-1 (1−101) in COS-7 cells. tHO-1 and caveolin-1 (1−101) were expressed in COS-7 cells. Cell lysates were separated by SDS-PAGE (4−12% gradient Bis-Tris gel) and analyzed by Western blotting as described in the Experimental Procedures. (A) The control lane indicates the COS-7 cells treated with only the transfection reagent. The tHO-1 and caveolin-1 (1−101) lanes indicate the COS-7 cells transfected with tHO-1 and caveolin-1 (1−101) expression vectors, respectively. Protein bands were visualized with the aid of anti-HO-1 (upper panel) and anti-caveolin-1 (middle panel) antibodies, respectively. The membrane of the middle panel was treated with WB stripping solution (Nacarai Tesque, Japan) to strip the anti-caveolin-1 antibody and reprobed with anti-polyhistidine antibody to visualize the His_6-tagged caveolin-1 (1−101) (lower panel). (B) The cell lysates from COS-7 cells transfected with caveolin-1 (1−101) expression vector (left lane) and tHO-1 plus caveolin-1 (1−101) expression vectors (right lane) were immunoprecipitated with anti-caveolin-1 antibody-conjugated beads (upper panel) and anti-HO-1 antibody-conjugated beads (lower panel), respectively. The precipitated proteins were separated by SDS-PAGE as in (A) and visualized with the aid of anti-HO-1 (upper panel) and anti-caveolin-1 antibodies (lower panel).

assume a complex tertiary structure.[43] In fact, caveolin-1 (1−101) purified from inclusion bodies treated with 8 M urea appeared to be fully interactive with tHO-1 and was used satisfactorily in all of the experiments in this study (see Figure 2).

Interaction between Coexpressed tHO-1 and Caveolin-1 (1−101) in Mammalian Cells. To probe the interaction between HO-1 and caveolin-1 in the cytoplasmic environment, immunoprecipitation experiments were attempted. First, expression vectors encoding tHO-1 and caveolin-1 (1−101) were separately transfected into COS-7 cells. The expression of the proteins was confirmed by Western blotting. tHO-1 was detected only in the cells transfected tHO-1 gene (Figure 1A, upper panel). On the other hand, the anti-caveolin-1 antibody detected major bands at ∼20 kDa for endogenous caveolin-1 in the control, tHO-1- and caveolin-1 (1−101)-gene transfected cells, respectively (Figure 1A, middle panel). In caveolin-1 (1−101)-gene transfected cells, overexpression of caveolin-1 (1−101) should be detected as a band of 16.8 kDa, which is calculated from the cDNA sequence plus extra 47 amino acid residues (His_6-tag and V5 epitope) derived from the expression vector. Under these conditions, however, it seems to be difficult to detect endogenous caveolin-1 (20.6 kDa) and caveolin-1 (1−101) as two distinct bands, possibly because of overlap. Therefore, to confirm the overexpression of caveolin-1 (1−101), the membrane of the middle panel of Figure 1A was reprobed with anti-polyhistidine antibody after stripping the anti-caveolin-1 antibody (Figure 1A, lower panel). As expected, expression of the His_6-tagged caveolin-1 (1−101) was detected only in the cells transfected with caveolin-1 (1−101) gene at the position corresponding to the lower part of the endogenous caveolin-1 band (compare the middle and lower panels of Figure 1A).

Results of the immunoprecipitation experiment are shown in Figure 1B. Cells transfected with caveolin-1 (1−101) gene alone were used as a control. When the control lysate was immunoprecipitated with either anti-HO-1 or anti-caveolin-1 antibodies, no distinctive immunoprecipitant was detected (Figure 1B, left lanes, upper and lower panels). In contrast, with the cells cotransfected with tHO-1 and caveolin-1 (1−101) genes, tHO-1 was detected in the eluent recovered after immunoprecipitation with anti-caveolin-1 antibody and caveolin-1 was also coprecipitated with anti-HO-1 antibody (Figure 1B, right lanes, upper and lower panels, respectively). The results indicate that tHO-1 directly associates with caveolin-1 (1−101) in the cytoplasmic environment.

Effect of Caveolin-1 (1−101) on the Enzymatic Activity of tHO-1. Effect of caveolin-1 (1−101) on the enzymatic activity of tHO-1 was examined to clarify whether or not caveolin-1 is able to regulate HO activity. As shown in left panel of Figure 2, the HO activity of tHO-1 was suppressed by caveolin-1 (1−101) in a dose-dependent manner. About 80% of HO activity was suppressed in the presence of 5 μM caveolin-1 (1−101). The tHO-1 mutant, F207A/F214A, showed no HO activity (Figure 2, right column). F207A and F214A exhibited 4 and 57% of the tHO-1 activity, respectively.

Inhibition of tHO-1 by Direct Binding of CAV(82−101). It is known that a 20-amino acid sequence, which is located in the membrane-proximal side of the N-terminal cytosolic domain of caveolin-1 (82−101 residues, DGIWKASFTTFTVTKYWFYR) (Figure 3A), modulates the function of various signaling proteins.[23−27,34−36] Hence, we investigated the interaction between tHO-1 and caveolin-1 with the synthetic peptide of this segment, designated as CAV(82−101). In the first step, *in vitro* binding was examined; tHO-1 was bound to the Cys-Ahx-CAV(82−101)-immobilized Sepharose beads, whereas L-Cys-immobilized beads did not bind tHO-1 (Figure 3B).

Next, enzyme kinetics of HO activity were analyzed in the presence and absence of CAV(82−101). As shown in

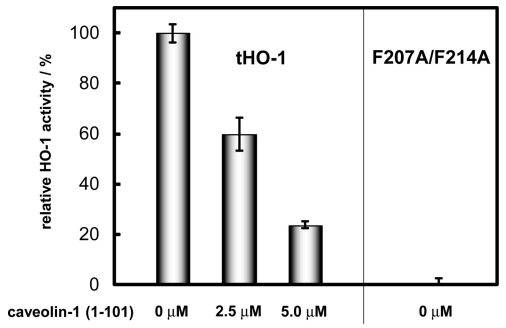

Figure 2. Effect of caveolin-1 (1−101) on HO activity of tHO-1. HO activity was measured as described in the Experimental Procedures. Left panel: tHO-1 (0.38 μM) was preincubated with 0, 2.5, and 5.0 μM caveolin-1 (1−101) at 4 °C for 30 min, and then its activity was measured. Right panel: HO activity of F207A/F214A (0.38 μM) in the absence of caveolin-1 (1−101).

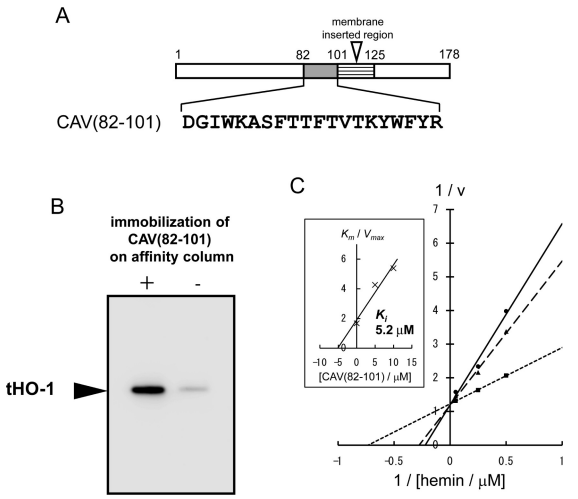

Figure 3. Interaction of tHO-1 and CAV(82−101). (A) The structure of rat caveolin-1 and the amino acid sequence of CAV(82−101). (B) *In vitro* binding assay of tHO-1 to CAV(82−101). tHO-1 was applied onto the Cys-Ahx-CAV(82−101)-immobilized (left lane) or L-Cys-immobilized column (right lane). The protein eluted with 6 M urea was separated by SDS-PAGE and visualized with the aid of anti-HO-1 antibody. (C) Lineweaver−Burk plot of the HO activity of tHO-1 in the presence of 0 μM (dotted line), 5 μM (dashed line), and 10 μM (solid line) CAV(82−101). Inset: the inhibition constant (K_i) of CAV(82−101) was estimated from the Dixon plot.

Figure 3C, the Lineweaver−Burk plot indicated that CAV(82−101) is a competitive inhibitor against the substrate hemin; the inhibition constant (K_i) was estimated to be 5.2 μM from the Dixon plot (inset of Figure 3C).

Interference with Heme−HO-1 Complex Formation by CAV(82−101). On the basis of the result that CAV(82−101) inhibits the HO activity of tHO-1 in a competitive manner, we then investigated the effect of CAV(82−101) on formation of heme−HO-1 complex by titration of tHO-1 with hemin. UV/vis spectral changes during titration are presented in Figure 4A. In the absence of CAV(82−101), the Soret peak at 405 nm, indicative of formation of heme−HO-1 complex, increased smoothly as hemin was added. However, its formation was clearly suppressed in the presence of 50 μM CAV(82−101); the absorbance around 340 nm indicates the accumulation of free hemin. Figure 4B shows the replots of $Abs_{405-340\ nm}$ versus hemin concentration during titrations with varied concentrations of CAV(82−101). In the absence of CAV(82−101), tHO-1 appeared to be saturated at about 7 μM hemin. When CAV(82−101) was present, the saturation points were clearly shifted to a higher hemin concentration.

Identification of Caveolin Binding Region in HO-1. To determine the caveolin binding motif in HO-1, affinities of tHO-1 mutants, F207A, F214A, and F207A/F214A to CAV(82−101) were compared with that of tHO-1 by SPR. Figure 5 shows association and dissociation curves of tHO-1 and these mutants against CAV(82−101) on SPR sensor chip. The tHO-1 exhibited unequivocal affinity to CAV(82−101); calculated K_D was 1.0×10^{-6} M. On the other hand, affinities of F207A, F214A, or F207A/F214A to CAV(82−101) were completely lost. There was little conformational difference between tHO-1 and F207A/F214A on circular dichroism spectra (data not shown). Although the identified caveolin binding motif in tHO-1 (FLLNIELF) is incomplete compared to the proposed motifs containing three aromatic amino acids,[23] our findings indicate that the aromatic residues in the motif (Phe^{207} and Phe^{214}) are deeply involved in binding to caveolin-1.

Determination of Minimum Sequence in CAV(82−101) for Inhibition of tHO-1 Activity. To specify a minimum sequence required for HO inhibition, CAV(82−101) was divided into the three 10-residue fragments (Figure 6A). Among these fragments, CAV(92−101) showed the strongest inhibitory effect, but the effects of CAV(82−91) and CAV(87−96) were only marginal (Figure 6B). Furthermore, the five-residue fragment, CAV(97−101), exerted an inhibitory effect comparable with CAV(92−101). Thus, at present, this five-residue segment is considered to be a minimum sequence for the interaction of caveolin-1 with tHO-1.

DISCUSSION

Caveolin-1 interacts with many signaling molecules in mammalian cells, including G-protein α-subunit,[25] Src kinase,[26] epidermal growth factor receptor,[24] Toll-like receptor 4,[28] and NOS.[31−33] Recently, Kim et al. reported that caveolin-1 physically interacts with HO-1.[16,17] In the present study, we first confirmed by immunoprecipitation experiments that tHO-1 and caveolin-1 (1−101) directly interact with each other (Figure 1B) and that the enzymatic activity of tHO-1 is effectively inhibited by caveolin-1 (1−101) (Figure 2), suggesting that downregulation of HO-1 by caveolin-1 takes place in mammalian cells.[16,17]

The 82−101 residues of caveolin-1, called "caveolin scaffolding domain",[23] has been reported to play an essential role in caveolin-related protein−protein interactions.[23−27,34−36] Actually the tHO-1 activity is inhibited by CAV(82−101) in a competitive manner with hemin (Figure 3C), and the hemin titration experiment showed that CAV(82−101) interferes with hemin binding to tHO-1 (Figure 4). The enzyme kinetics and SPR experiments gave the comparable K_i and K_D values of 5.2 and 1.0 μM for CAV(82−101), respectively (Figures 3C and 5). These observations indicated that CAV(82−101) and hemin share a common binding site within the tHO-1 protein. The identified caveolin binding motif (FLLNIELF) of rat HO-1 is incomplete compared to the proposed consensus sequence.[23] The affinity between tHO-1 and CAV(82−101), however, was totally lost or remarkably eliminated by replacement of Phe^{207}

dx.doi.org/10.1021/bi200601t | *Biochemistry* 2011, 50, 6824−6831

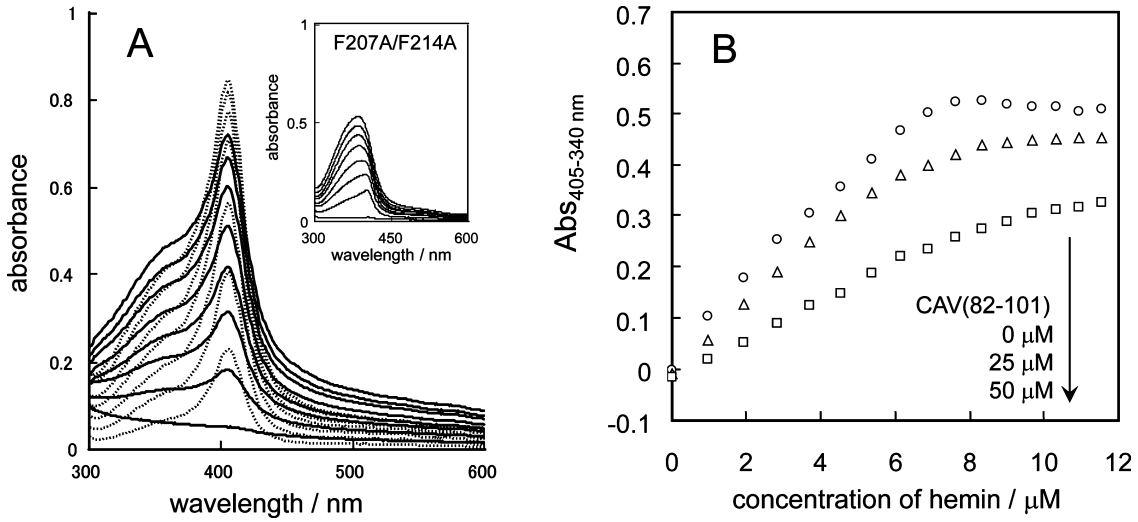

Figure 4. Interference of heme−HO-1 complex formation by CAV(82−101). (A) Titration of tHO-1 (5 μM) with hemin was carried out in the presence (solid lines) and absence (dotted lines) of 50 μM CAV(82−101) as described in the Experimental Procedures. The hemin concentration ranged from 0 to 11.5 μM. Inset: the spectral change during titration of F207A/F214A (5 μM) with hemin in the absence of CAV(82−101). (B) The replots of the Soret band intensity ($Abs_{405-340\ nm}$) versus hemin concentration in the presence of 0 μM (circles), 25 μM (triangles), and 50 μM (squares) CAV(82−101).

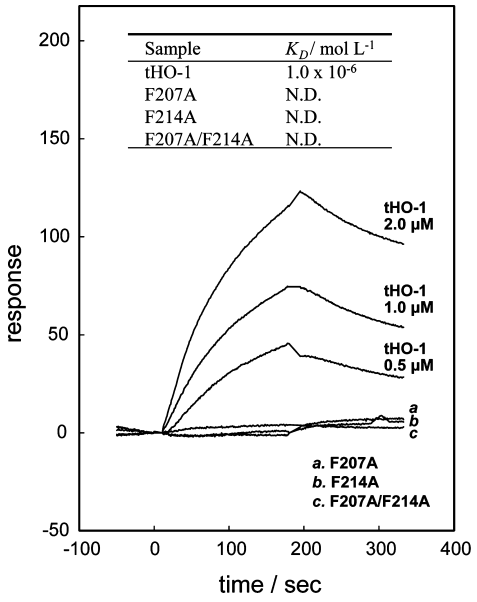

Figure 5. SPR signals generated from interaction of tHO-1 with CAV(82−101). SPR measurements were carried out as described in the Experimental Procedures. tHO-1 (0.5, 1.0, and 2.0 μM) and 2.0 μM each of F207A (a), F214A (b), or F207A/F214A (c) were injected on to the CAV(82−101)-immobilized sensor chip. The dissociation constants (K_D) are shown in the table. N.D.: not detected.

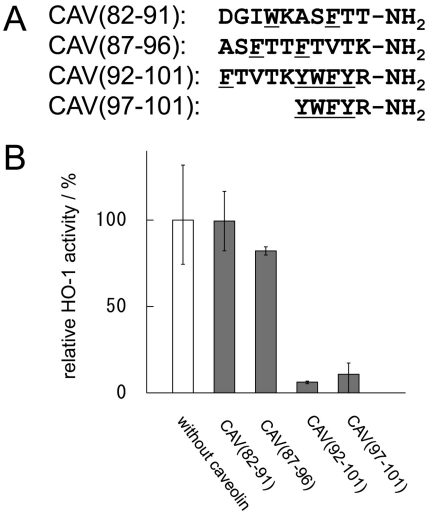

Figure 6. Inhibition of the HO activity of tHO-1 by the fragment peptides of CAV(82−101). (A) Primary structures of the fragment peptides of CAV(82−101). Aromatic amino acids are underlined. (B) Effects of the fragment peptides on the activity of tHO-1. The HO activity was measured as described in the Experimental Procedures. tHO-1 dissolved in the assay mixture was preincubated with the peptides indicated (100 μM) at 4 °C for 30 min.

and/or Phe^{214} (Figure 5) with Ala, strongly indicating that HO-1 binds to caveolin-1 via this motif.

Our previous X-ray analysis of rat HO-1 crystals revealed that the enzyme is composed of eight α-helical domains (A−H helices).[44,45] Phe^{207} and Phe^{214} are localized at the central part of H helix (Pro^{193}−Thr^{222}), and the two aromatic side chains of these residues are oriented toward the inside of the heme pocket. The aromatic side chains are in contact with heme; namely, the side chain of Phe^{207} is located under the β-meso edge of heme, and Phe^{214} forms part of a hydrophobic wall opposite the α-meso edge (Figure 7).[46] In fact, the Soret band at 405 nm, indicative of heme−HO-1 complex formation, was not observed during the hemin titration with F207A/F214A (inset of Figure 4A). The complete loss of the HO activity of F207A/F214A (right column of Figure 2) should be additional evidence that these residues are essential for the binding of heme.

The principle behind HO-1−caveolin-1 complex formation is biophysically interesting. CAV(87−96) and CAV(92−101) share an overlapped sequence (92−96 residues), but only CAV(92−101) exhibited an inhibitory effect on HO-1 activity (Figure 6B). Surprisingly, CAV(97−101), a C-terminal five-residue sequence of CAV(92−101), was able to inhibit the HO-1 activity to a similar extent compared to CAV(92−101).

dx.doi.org/10.1021/bi200601t | *Biochemistry* 2011, 50, 6824−6831

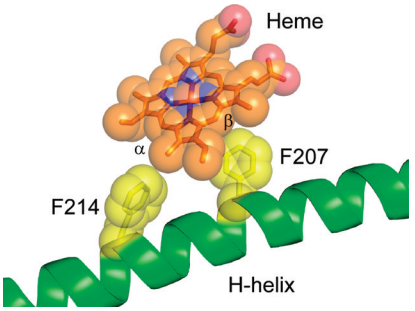

Figure 7. Location of Phe^{207} and Phe^{214} in the crystal structure of heme−HO-1 complex. Phe^{207} and Phe^{214} (yellow) reside in the central portion of "H-helix", and their aromatic side chains are in contact with heme (orange) in the heme pocket.[44]

Of interest is that the content of aromatic residues of CAV(97−101) is high, comprising 4 of the 5 amino acids (Figure 6A). As stated above, replacement of the aromatic amino acids in the caveolin binding motif of tHO-1 resulted in the loss of affinity of tHO-1 to CAV(82−101) (Figure 5). These observations suggest that these aromatic residues in caveolin-1 and HO-1 play key roles in the association of both proteins. It is conceivable that the $\pi-\pi$ stacking chemistry and hydrophobic interaction between the aromatic residues of both proteins are the driving forces for binding of the two proteins.

Couet et al. reported that C-terminal 16 residues of the caveolin scaffolding domain (residues 86−101) are the minimum requisite for binding of caveolin-1 to G protein α-subunit. But the peptide corresponding to CAV(92−101) failed to bind to G protein α-subunit.[23] As well, the peptide from 90 to 101 residues of caveolin-1 did not exhibit an inhibitory effect on NOS activity.[34] As shown in the present study, the HO-1 activity was inhibited only by the C-terminal five-residue stretch of the caveolin scaffolding domain (97−101 residues). This variation in interaction with caveolin-1 indicates that modulating mechanisms by caveolin-1 differ among caveolin-1-interacting proteins. These differences may provide a clue for development of an HO specific inhibitor; namely, the caveolin-derived peptides used in this study and their related peptides should be candidate proteineous HO inhibitors.

The reductase domain of NOS, which does not have a caveolin binding motif, interacts with caveolin-1.[35,36] The binding of caveolin-1 compromises the ability of NOS to bind calmodulin and to donate electrons to the heme. In the CPR-supported HO reaction, CPR must associate with HO for electron transfer.[41,47] Interaction between caveolin and CPR is expected based on the similarity between the NOS and HO reactions. Studies along this line are ongoing in our laboratory.

In summary, we confirmed the direct interaction between HO-1 and caveolin-1 and found that caveolin-1 is a competitive inhibitor of HO-1 with heme. A five-amino acid sequence (residues 97−101) in caveolin-1 was identified as a minimum sequence for binding to HO-1.

AUTHOR INFORMATION

Corresponding Author

*Tel +81-942-31-7536; Fax +81-942-31-7839; e-mail higashiy@med.kurume-u.ac.jp.

Funding

This work was supported in part by Grants-in-Aid for Young Scientists (B) (21770152, 20770092, and 20790343) and a Grant-in-Aid for Scientific Research (C) (21590321) from the Ministry of Education, Culture, Sports, Science, and Technology of Japan.

ACKNOWLEDGMENTS

We are grateful to Mr. T. Ishikawa of Fukuoka Industrial Technology Center for the use of MALDI-TOF MS.

ABBREVIATIONS

Ahx, 6-aminohexanoic acid; BVR, biliverdin reductase; CO, carbon monoxide; CPR, NADPH−cytochrome P450 reductase; Fmoc, 9-fluorenylmethoxycarbonyl; HO, heme oxygenase; HRP, horseradish peroxidase; NO, nitric oxide; NOS, NO synthase; sGC, soluble guanylyl cyclase; SPR, surface plasmon resonance.

REFERENCES

(1) Ortiz de Montellano, P. R., and Auclair, K. (2003) Heme Oxygenase Structure and Mechanism, in *Porphyrin Handbook* (Kadish, K., Smith, K., and Guilard, R., Eds.) Vol. *12*, pp 183−210, Academic Press, New York.

(2) Ortiz de Montellano, P. R. (2000) The mechanism of heme oxygenase. *Curr. Opin. Chem. Biol. 4*, 221−227.

(3) Tenhunen, R., Marver, H. S., and Schmid, R. (1969) Microsomal heme oxygenase. Characterization of the enzyme. *J. Biol. Chem. 244*, 6388−6394.

(4) Yoshida, T., Noguchi, M., and Kikuchi, G. (1980) Oxygenated form of heme. heme oxygenase complex and requirement for second electron to initiate heme degradation from the oxygenated complex. *J. Biol. Chem. 255*, 4418−4420.

(5) Schacter, B. A., Nelson, E. B., Marver, H. S., and Masters, B. S. (1972) Immunochemical evidence for an association of heme oxygenase with the microsomal electron transport system. *J. Biol. Chem. 247*, 3601−3607.

(6) Tenhunen, R., Marver, H. S., and Schmid, R. (1968) The enzymatic conversion of heme to bilirubin by microsomal heme oxygenase. *Proc. Natl. Acad. Sci. U. S. A. 61*, 748−755.

(7) Trakshel, G. M., and Maines, M. D. (1989) Multiplicity of heme oxygenase isozymes. HO-1 and HO-2 are different molecular species in rat and rabbit. *J. Biol. Chem. 264*, 1323−1328.

(8) Shibahara, S., Yoshida, T., and Kikuchi, G. (1979) Mechanism of increase of heme oxygenase activity induced by hemin in cultured pig alveolar macrophages. *Arch. Biochem. Biophys. 197*, 607−617.

(9) Kharitonov, V. G., Sharma, V. S., Pilz, R. B., Magde, D., and Koesling, D. (1995) Basis of guanylate cyclase activation by carbon monoxide. *Proc. Natl. Acad. Sci. U. S. A. 92*, 2568−2571.

(10) Stone, J. R., and Marletta, M. A. (1994) Soluble guanylate cyclase from bovine lung: activation with nitric oxide and carbon monoxide and spectral characterization of the ferrous and ferric states. *Biochemistry 33*, 5636−5640.

(11) Ryter, S. W., Otterbein, L. E., Morse, D., and Choi, A. M. (2002) Heme oxygenase/carbon monoxide signaling pathways: regulation and functional significance. *Mol. Cell. Biochem. 234−235*, 249−263.

(12) Ryter, S. W., Morse, D., and Choi, A. M. (2004) Carbon monoxide: to boldly go where NO has gone before. *Sci. STKE 2004*, RE6.

(13) Wang, X., Wang, Y., Kim, H. P., Nakahira, K., Ryter, S. W., and Choi, A. M. (2007) Carbon monoxide protects against hyperoxia-induced endothelial cell apoptosis by inhibiting reactive oxygen species formation. *J. Biol. Chem. 282*, 1718−1726.

(14) Maruhashi, K., Kasahara, Y., Ohta, K., Wada, T., Nakamura, N., Toma, T., Koizumi, S., and Yachie, A. (2004) Paradoxical enhancement of oxidative cell injury by overexpression of heme oxygenase-1 in an anchorage-dependent cell ECV304. *J. Cell. Biochem. 93*, 552−562.

(15) Suttner, D.M., and Dennery, P. A. (1999) Reversal of HO-1 related cytoprotection with increased expression is due to reactive iron. *FASEB J. 13*, 1800−1809.

(16) Jung, N. H., Kim, H. P., Kim, B. R., Cha, S. H., Kim, G. A., Ha, H., Na, Y. E., and Cha, Y. N. (2003) Evidence for heme oxygenase-1 association with caveolin-1 and −2 in mouse mesangial cells. *IUBMB Life 55*, 525−532.

(17) Kim, H. P., Wang, X., Galbiati, F., Ryter, S. W., and Choi, A. M. (2004) Caveolae compartmentalization of heme oxygenase-1 in endothelial cells. *FASEB J. 18*, 1080−1089.

(18) Kurzchalia, T. V., Dupree, P., Parton, R. G., Kellner, R., Virta, H., Lehnert, M., and Simons, K. (1992) VIP21, a 21-kD membrane protein is an integral component of trans-Golgi-network-derived transport vesicles. *J. Cell. Biol. 118*, 1003−1014.

(19) Scherer, P. E., Okamoto, T., Chun, M., Nishimoto, I., Lodish, H. F., and Lisanti, M. P. (1996) Identification, sequence, and expression of caveolin-2 defines a caveolin gene family. *Proc. Natl. Acad. Sci. U. S. A. 93*, 131−135.

(20) Song, K. S., Scherer, P. E., Tang, Z., Okamoto, T., Li, S., Chafel, M., Chu, C., Kohtz, D. S., and Lisanti, M. P. (1996) Expression of caveolin-3 in skeletal, cardiac, and smooth muscle cells. Caveolin-3 is a component of the sarcolemma and co-fractionates with dystrophin and dystrophin-associated glycoproteins. *J. Biol. Chem. 271*, 15160−15165.

(21) Okamoto, T., Schlegel, A., Scherer, P. E., and Lisanti, M. P. (1998) Caveolins, a family of scaffolding proteins for organizing "preassembled signaling complexes" at the plasma membrane. *J. Biol. Chem. 273*, 5419−5422.

(22) Smart, E. J., Graf, G. A., McNiven, M. A., Sessa, W. C., Engelman, J. A., Scherer, P. E., Okamoto, T., and Lisanti, M. P. (1999) Caveolins, liquid-ordered domains, and signal transduction. *Mol. Cell. Biol. 19*, 7289−7304.

(23) Couet, J., Li, S., Okamoto, T., Ikezu, T., and Lisanti, M. P. (1997) Identification of peptide and protein ligands for the caveolin-scaffolding domain. Implications for the interaction of caveolin with caveolae-associated proteins. *J. Biol. Chem. 272*, 6525−6533.

(24) Couet, J., Sargiacomo, M., and Lisanti, M. P. (1997) Interaction of a receptor tyrosine kinase, EGF-R, with caveolins. Caveolin binding negatively regulates tyrosine and serine/threonine kinase activities. *J. Biol. Chem. 272*, 30429−30438.

(25) Li, S., Okamoto, T., Chun, M., Sargiacomo, M., Casanova, J. E., Hansen, S. H., Nishimoto, I., and Lisanti, M. P. (1995) Evidence for a regulated interaction between heterotrimeric G proteins and caveolin. *J. Biol. Chem. 270*, 15693−15701.

(26) Li, S., Couet, J., and Lisanti, M. P. (1996) Src tyrosine kinases, G_α subunits, and H-Ras share a common membrane-anchored scaffolding protein, caveolin. Caveolin binding negatively regulates the auto-activation of Src tyrosine kinases. *J. Biol. Chem. 271*, 29182−29190.

(27) Ju, H., Zou, R., Venema, V. J., and Venema, R. C. (1997) Direct interaction of endothelial nitric-oxide synthase and caveolin-1 inhibits synthase activity. *J. Biol. Chem. 272*, 18522−18525.

(28) Wang, X. M., Kim, H. P., Nakahira, K., Ryter, S. W., and Choi, A. M. (2009) The heme oxygenase-1/carbon monoxide pathway suppresses TLR4 signaling by regulating the interaction of TLR4 with caveolin-1. *J. Immunol. 182*, 3809−3818.

(29) Kim, H. P., Wang, X., Nakao, A., Kim, S. I., Murase, N., Choi, M. E., Ryter, S. W., and Choi, A. M. (2005) Caveolin-1 expression by means of p38β mitogen-activated protein kinase mediates the antiproliferative effect of carbon monoxide. *Proc. Natl. Acad. Sci. U. S. A. 102*, 11319−11324.

(30) Kim, H. P., Ryter, S. W., and Choi, A. M. (2006) CO as a cellular signaling molecule. *Annu. Rev. Pharmacol. Toxicol. 46*, 411−449.

(31) Venema, V.J., Zou, R., Ju, H., Marrero, M. B., and Venema, R. C. (1997) Caveolin-1 detergent solubility and association with endothelial nitric oxide synthase is modulated by tyrosine phosphorylation. *Biochem. Biophys. Res. Commun. 236*, 155−161.

(32) Venema, R.C., Ju, H., Zou, R., Ryan, J. W., and Venema, V. J. (1997) Subunit interactions of endothelial nitric-oxide synthase. Comparisons to the neuronal and inducible nitric-oxide synthase isoforms. *J. Biol. Chem. 272*, 1276−1282.

(33) Venema, V. J., Ju, H., Zou, R., and Venema, R. C. (1997) Interaction of neuronal nitric-oxide synthase with caveolin-3 in skeletal muscle. Identification of a novel caveolin scaffolding/inhibitory domain. *J. Biol. Chem. 272*, 28187−28190.

(34) Garcia-Cardena, G., Martasek, P., Masters, B. S., Skidd, P. M., Couet, J., Li, S., Lisanti, M. P., and Sessa, W. C. (1997) Dissecting the interaction between nitric oxide synthase (NOS) and caveolin. Functional significance of the NOS caveolin binding domain *in vivo*. *J. Biol. Chem. 272*, 25437−25440.

(35) Ghosh, S., Gachhui, R., Crooks, C., Wu, C., Lisanti, M. P., and Stuehr, D. J. (1998) Interaction between caveolin-1 and the reductase domain of endothelial nitric-oxide synthase. Consequences for catalysis. *J. Biol. Chem. 273*, 22267−22271.

(36) Sato, Y., Sagami, I., and Shimizu, T. (2004) Identification of caveolin-1-interacting sites in neuronal nitric-oxide synthase. Molecular mechanism for inhibition of NO formation. *J. Biol. Chem. 279*, 8827−8836.

(37) Taira, J., Jelokhani-Niaraki, M., Osada, S., Kato, F., and Kodama, H. (2008) Ion-channel formation assisted by electrostatic interhelical interactions in covalently dimerized amphiphilic helical peptides. *Biochemistry 47*, 3705−3714.

(38) Hidaka, T., Omata, Y., and Noguchi, M. (1996) Cloning and expression of cDNA for soluble form of rat heme oxygenase-1. *Kurume Med. J. 43*, 313−324.

(39) Yoshida, T., and Kikuchi, G. (1978) Purification and properties of heme oxygenase from pig spleen microsomes. *J. Biol. Chem. 253*, 4224−4229.

(40) Smith, K. M. (1975) *Porphyrins and Metalloporphyrins*, Elsevier, Amsterdam.

(41) Higashimoto, Y., Sakamoto, H., Hayashi, S., Sugishima, M., Fukuyama, K., Palmer, G., and Noguchi, M. (2005) Involvement of NADPH in the interaction between heme oxygenase-1 and cytochrome P450 reductase. *J. Biol. Chem. 280*, 729−737.

(42) Sargiacomo, M., Scherer, P. E., Tang, Z., Kubler, E., Song, K. S., Sanders, M. C., and Lisanti, M. P. (1995) Oligomeric structure of caveolin: implications for caveolae membrane organization. *Proc. Natl. Acad. Sci. U. S. A. 92*, 9407−9411.

(43) Fernandez, I., Ying, Y., Albanesi, J., and Anderson, R. G. (2002) Mechanism of caveolin filament assembly. *Proc. Natl. Acad. Sci. U. S. A. 99*, 11193−11198.

(44) Sugishima, M., Omata, Y., Kakuta, Y., Sakamoto, H., Noguchi, M., and Fukuyama, K. (2000) Crystal structure of rat heme oxygenase-1 in complex with heme. *FEBS Lett. 471*, 61−66.

(45) Schuller, D.J., Wilks, A., Ortiz de Montellano, P. R., and Poulos, T. L. (1999) Crystal structure of human heme oxygenase-1. *Nat. Struct. Biol. 6*, 860−867.

(46) Sugishima, M., Sakamoto, H., Kakuta, Y., Omata, Y., Hayashi, S., Noguchi, M., and Fukuyama, K. (2002) Crystal structure of rat apo-heme oxygenase-1 (HO-1): mechanism of heme binding in HO-1 inferred from structural comparison of the apo and heme complex forms. *Biochemistry 41*, 7293−7300.

(47) Wang, J., and Ortiz de Montellano, P. R. (2003) The binding sites on human heme oxygenase-1 for cytochrome p450 reductase and biliverdin reductase. *J. Biol. Chem. 278*, 20069−20076.